Metabolomics Coupled with Integrated Approach Reveals the Therapeutic Effect of Higenamine Combined with [6]-Gingerol on Doxorubicin - Induced Chronic Heart Failure in Rats

Jianxia Wen (wenjx2048@126.com)
Chengdu University of Traditional Chinese Medicine https://orcid.org/0000-0002-1184-8758
Xiao Ma
Chengdu University of Traditional Chinese Medicine
Mingjie Li
Guizhou Medical University
Ming Niu
Chinese PLA General Hospital
Ying Huang
Chinese PLA General Hospital
Junjie Hao
Chinese PLA General Hospital
Ruilin Wang
Chinese PLA General Hospital
Ruisheng Li
Chinese PLA General Hospital
Yanling Zhao
Chinese PLA General Hospital
Jian Wang
Chengdu University of Traditional Chinese Medicine

Research

Keywords: Higenamine, [6]-gingerol, metabolomics, chronic heart failure, energy metabolism, doxorubicin

Posted Date: June 1st, 2020

DOI: https://doi.org/10.21203/rs.3.rs-31131/v1

Version of Record: A version of this preprint was published on November 17th, 2020. See the published version at https://doi.org/10.1186/s13020-020-00403-0.

Abstract

Background The combination of Aconiti Lateralis Radix Praeparata (ALRP) and Zingiberis Rhizoma (ZR) is one of the most typical representatives reflecting the very essence of the theory of Chinese material medica compatibility, which has been used to treat cardiovascular disease for many years. Previously, we demonstrated that ALRP-ZR prevented doxorubicin (DOX)-induced chronic heart failure (CHF) *in vivo*. However, its active components are still unclear. This study was aimed to investigate the therapeutic effect and potential mechanism of higenamine combined with [6]-gingerol (HG/[6]-GR) against doxorubicin (DOX) - induced chronic heart failure (CHF) in rats.

Methods Therapeutic effects of HG/[6]-GR on hemodynamics indices, serum biochemical indicators, histopathology and TUNEL staining of rats were assessed. Moreover, a UHPLC-Q-TOF/MS-based serum metabolomic approach coupled with biochemical assay had been performed to identify the potential mechanisms of HG/[6]-GR on DOX-induced CHF.

Results HG/[6]-GR had effects on promoting of hemodynamic indices, decreasing serum biochemical indicators, and alleviating histological damage of heart tissue. Serum metabolomics analyses indicated that the therapeutic effects of HG and [6]-GR were mainly associated with the regulation of eight metabolites and twelve pathways, which may be responsible for the therapeutic efficacy of HG/[6]-GR. Moreover, the results showed that HG/[6]-GR could substantially regulate the expression level of energy metabolism-related metabolites and pathways.

Conclusions Multivariate statistical analysis has provided new insights for understanding CHF and investigating the therapeutic effects and mechanisms of HG/[6]-GR, which influencing the metabolites related to energy metabolism pathway *via* metabolomics.

Background

Cardiovascular disease (CVD) causes a huge health and economic burden in the United States and the world. According to the data of National Health and Nutrition Examination Survey from 2013 to 2016, the prevalence of CVD in adults ≥ 20 years is 48.0% in total, and the prevalence is increasing with advancing age in both males and females.[1] Chronic heart failure (CHF) is the terminal stage of various heart diseases, which remains a major clinical cause of morbidity, mortality and seriously endangers the health of humans globally.[2] It is a common cause of death with high direct and indirect treatment costs.[3] Currently, the problems faced by patients and medical community are high mortality, repeated hospitalization and combined therapies. The different kinds of pharmacological agents used for patients with CHF include angiotensin-converting enzyme inhibitors (ACEI), aldosterone antagonists, angiotensin-receptor blockers, aldosterone antagonists, β-blockers, inotropic agents, diuretics, digitalis, nitrates, vasodilators and so on.[4,5] Although these agents are all major treatments, its poor prognosis and few therapeutic options make CHF still a growing global public health concern. The prevention and treatment of CHF remains major issues globally.[6]

Natural medicine has the characteristics of various component and complex mechanism, which has great potential in multiple disease treatment. Simultaneously, these products can act at multiple targets and pathways in the complex pathogenesis of diseases. In the prevention and treatment of CHF, traditional Chinese medicine (TCM) plays a special advantage with its multi-components, multi-target and multi-channel. Our previous studies have shown that the compatibility use of higenamine (HG, one of the active compounds of Aconiti Lateralis Radix Praeparata) and 6-gingerol ([6]-GR, one of the active compounds of Zingiberis Rhizoma) inhibits doxorubicin (DOX)-

induced CHF *via* promoting mitochondrial energy metabolism.[6] However, the potential mechanism of HG combined with [6]-GR (HG/[6]-GR) for the treatment of CHF had not been comprehensively elucidated. It remains to be elucidated how HG/[6]-GR can prevent and treat CHF by affecting mitochondrial energy metabolism.

Metabolomics is a comprehensive and systematic study of small molecule metabolites in biological samples or organs.[7] It can characterize changes of endogenous metabolites and their organic relations with physiological and pathological phenotypes after disturbance.[8] The metabolism of organism changes its dynamic balance due to the occurrence of disease, so it is helpful to understand the metabolic mechanism of organism by analyzing the composition of body fluid through metabolomics and obtaining biomarkers changed by disease induction. One of the basic methods of metabolomics research is the combination of advanced modern analytical technology, pattern recognition and expert system.[9] In recent years, metabolomics has also been used to identify specific biomarkers and evaluate the role of TCM in various diseases.[10-12] Therefore, the objective of current study was to use serum metabolomic analysis accompanied by biochemical and histopathological approaches to investigate and verify the metabolic profiles of blood metabolite spectrum caused by the development of CHF, as well as the treatment of HG/[6]-GR. Simultaneously, this study was expected to reveal the anti-CHF mechanism of HG/[6]-GR in SD rats.

Materials And Methods

Materials

Standard products of HG (CAS No.: 5843-65-2; Cat No. CHB180121) and [6]-GR (CAS No.: 23513-14-6; Cat No. CHB180306) were obtained from Chroma Biotechnology Co. Ltd (Chengdu, China). DOX hydrochloride injection was purchased from Shenzhen Main Luck pharmaceutical Inc. (batch number: 1710E1, Shenzhen, China). Dobutamine hydrochloride (DH) injection (Batch number: 1803203, Shanghai, China) was purchased from SPH NO.1 Biochemical & Pharmaceutical CO., LTD.

Animal Handling

Male Sprague - Dawley (SD) rats (200 ± 10 g) were purchased from the Beijing Keyu Animal Breeding Center (Beijing, China) with a permission number of SCXK-(jing) 2018-0010. Rats were fed in the Fifth Medical Center of PLA General Hospital. Rats in the control group were intragastrically given normal saline. Simultaneously, rats in the other groups were given DOX hydrochloride injection in the doses of 2.5 mg/kg body weight twice a week for six times. Thus, the accumulative doses of DOX was 15 mg/kg body weight.[13-15] As for the judgment of CHF model, hemodynamic indices were comprehensively assessed by a RM6240 multi-channel physiological signal acquisition system (Chengdu Instrument Factory, Sichuan, China) as our previous studies.[16-19] When the values of $+dp/dt_{max}$ were reduced to 50% of the control group, CHF model was successfully prepared.

Forty rats with successfully prepared CHF model were randomly assigned into five groups of eight rats in each group: DOX group, DH positive group (50 μg/kg/d), HG group (5 mg/kg/d), [6]-GR group (5 mg/kg/d), and HG/[6]-GR compatibility group (10 mg/kg/d). All rats were intraperitoneally injected with corresponding drugs once a day for seven consecutive days. It should be noted that CHF rats intraperitoneally injected with 5 mg/kg/d HG and [6]-GR showed a good therapeutic effect in our previous study.[20] Hemodynamic indices were assessed after the final

injection. All animals were sacrificed to collect serum samples and cardiac tissues for HE staining, TUNEL staining, and metabolomic analysis.

Detection of pharmacodynamic indices

Serum biochemical indices, including BNP, NT-proBNP, LDH, CK-MB, and AST were determined on a Synergy hybrid reader (Biotek, Winooski, USA). Hematoxylin-eosin (H&E) staining was carried out for showing myocardial morphological changes. Terminal deoxynucleotidyl transferase dUTP nick end labeling (TUNEL) assay was performed to indicate the cytotoxicity, cell damage and its recovery. Left ventricular myocardial tissue of rats was cut longitudinally. Next, cardiac tissue were fixed with 4% paraformaldehyde solution and embedded in paraffin for pathological observation. All the sections were observed under a Nikon microscope and analyzed by a Pro-Plus 7200 software.

Preparation of serum metabolomics samples

Firstly, the serum samples were thawed at 4°C. 200 μL of the serum was mixed with 600 μL of methanol to precipitate the protein. After centrifugation (13,800 g, 4℃, 10 min), the supernatant was transferred into a polypropylene tube and filtered *via* a syringe filter (0.22 μm) for obtaining the injection sample. Simultaneously, to assess the stability and reproducibility of serum metabolomics samples, the quality control (QC) sample was prepared by mixing all individual samples with10 uL aliquots in each.

Chromatography analysis

The serum samples were measured on an Agilent 1290 series UHPLC system (Agilent Technologies, Santa Clara, USA) coupled with a ZORBAX RRHD 300 SB-C18 column (100 × 2.1 mm, 1.8-μm, Agilent Technologies, Santa Clara, USA) for chromatography and separation. During the analysis, the setting conditions were as follows: sample maintaining temperature, 4 °C; injection volume: 4 μL; column temperature: 30 °C; flow rate, 0.30 mL/min. The mobile phases were composed as solvent A (0.1% formic acid in acetonitrile), and solvent B (0.1% formic acid in water). The gradient elution was set as Table 1. To ensure the stability and repeatability of the UHPLC-Q-TOF/MS systems, QC sample was injected followed by a blank sample after each injecting.

Mass spectrometry analysis

Mass spectrometry analysis was performed using an Agilent 6550A Q-TOF/MS instrument (Agilent Technologies, Santa Clara, USA) coupled with an electrospray ionization (ESI) source in both positive and negative ionization mode in the full scan mode (80 - 1200 m/z). The setting conditions in mass spectrometry analysis were as follows: gas temperature: 225 °C in positive ionization mode and 200 °C in negative ionization mode; nozzle voltage: 500 V in both positive and negative mode; electrospray capillary voltage, 4.0 kV in positive ionization mode and 3.0 kV in negative ionization mode; nebulizer: 45 pisg (positive) and 35 pisg (negative); gas flow rare: 11 L/min; mass range: from 80 to 1000 m/z; sheath gas flow: 12 L/min; sheath gas temperature: 350 °C.

Data processing and multivariate data analysis

After statistical analysis by MetaboAnalyst 4.0 (http://www.MetaboAnalyst.ca/),[21] the raw data were converted into “data_normalized.csv” format. Then, the normalized file in positive mode and negative mode were imported into the SIMCA-P program (version 14.1, MKS Umetrics) for multivariate analysis. Principal component analysis (PCA) was performed after concentration and normalization to check the overall metabolism of each sample group, and observe sample aggregation, dispersion and abnormal values. Next, partial least-squares discriminant analysis (PLS-DA) was used to identify the main difference variables that caused the aggregation and discretization. Subsequently, 100 iteration permutation tests were performed to avoid the over-fitting of PLS-DA. Potential biomarkers were selected according to the parameters of variable VIP > 1 and |Pcorr| > 0.58 from PLS-DA. SPSS 23.0 software with the *t*-test was used to test the peak areas of differential metabolites and determine the differences of biomarkers between groups (p-value threshold was set at 0.05).

Potential metabolites identification and pathway analysis

Furthermore, a MassHunter Profinder software (version B.06.00, Agilent, California, USA) was used to detect the sample data for peak detection and alignment. Full scan mode was employed and the mass range was 80 to 1000 m/z. The online biochemical database HMDB database (http://www.hmdb.ca/) and METLIN (http://metlin.scripps.edu/) were used to identify the potential metabolites. MetaboAnalyst 4.0 was used for the pathway analysis. Finally, to identify and visualize the affected metabolic pathways, the biomarkers were put into MetaboAnalyst 4.0 based on the pathway library of Rattus norvegicus (rat). In the present study, the bioactive components, possible biomarkers and potential mechanisms of HG and [6]-GR in the treatment of CHF induced by DOX were comprehensively elucidated using the serum metabolomics strategy.

Statistical analysis

All data were analyzed using SPSS 23.0 software program (Chicago, United States) and GraphPad Prism 8.2.0 software (GraphPad Software). The differences of data between groups were assessed by one-way analysis of variance (ANOVA). Values in the text were presented as mean ± SD. $P < 0.05$ was considered statistically significant. $P < 0.01$ was considered highly significant.

Results

Hemodynamics indices

The results in Table 2 showed that DOX could substantially decrease the LVSP and $+dp/dt_{max}$ value while significantly increase the LVEDP and $-dp/dt_{max}$ value. Notably, the $+dp/dt_{max}$ value had reduced to 50% of the control group, indicating that the model of CHF was successfully prepared. In addition, the therapeutic effects of HG/[6]-GR on heart function was evaluated by assessing the hemodynamics indices. As shown in Figure 1, compared with the control group, the hemodynamic indices levels of LVSP and $+dp/dt_{max}$ in the DOX group were still decreased ($P < 0.01$). Simultaneously, compared with the DOX group, DH, HG, [6]-GR, and HG/[6]-GR could dramatically increase the levels of LVSP and $+dp/dt_{max}$ and decrease the LVEDP and $-dp/dt_{max}$ value. The order of the therapeutic effects was HG/[6]-GR > HG > [6]-GR. Also, compared with HG and [6]-GR used alone, HG/[6]-GR group had a more superior effect on increasing heart function (Figure 1).

Myocardial biomarkers

Serum levels of myocardial biomarkers were included in Figure 2. Serum levels of BNP, NT-proBNP, LDH, CK-MB, and AST in the DOX group were significantly increased (P 0.01) compared with the control group, which indicated the damage of heart function. However, compared with the DOX group, HG and [6]-GR could reduce the serum concentrations of these biomarkers. Notably, these biomarkers were substantially decreased in DH and HG/[6]-GR (P 0.01) group compared with the DOX group. Furthermore, HG/[6]-GR group was almost equal to the DH group, which markedly decreased the serum levels of BNP, NT-proBNP, LDH, CK-MB, and AST compare with HG or [6]-GR used alone ((P 0.05, P 0.01). Thus, [6]-GR might enhance the therapeutic role of HG in the treatment of CHF.

Histopathological changes

After administration, compared with the control group, the rats in DOX group had pathological changes such as widening and breaking of myocardial tissue space, vacuolar degeneration, edema, necrosis and atrophy of myocardial cells. Compared with the DOX group, the histopathology of HG and [6]-GR group was improved, but some rats still had widened and broken myocardial tissue space, vacuolation and degeneration of myocardial cells, while DH and HG/[6]-GR group showed significant improvement in cardiac pathology, less vacuolation, edema, necrosis, atrophy and other pathological changes of myocardial cells. The histopathological results (Figure 3) showed the degree of damage in each group.

Detection of cardiomyocyte apoptosis

TUNEL staining was used to detect the therapeutic effect of HG/[6]-GR on DOX induced cardiomyocyte apoptosis and its recovery. As shown in Figure 4, compared with the control group, the TUNEL positive proportion of cardiomyocytes in DOX treatment group increased significantly, indicating that DOX could cause cardiomyocyte apoptosis. In contrast, HG and [6]-GR used alone could reduce the apoptosis rate of cardiomyocytes in varying degrees. Moreover, HG/[6]-GR had a significant inhibitory effect on cardiomyocyte apoptosis, indicating that HG combined with [6]-GR had a synergistic anti apoptotic effects. These results showed that HG/[6]-GR had a significant protective effect on CHF myocardial tissue. The results clearly showed that the HG/[6]-GR could effectively alleviate CHF in rats.

Metabolic profile analysis

The metabolic profile analysis of serum samples was performed using UHPLC-Q-TOF/MS both in the positive and negative electrospray ionization (ESI) modes. PCA analysis was performed to assess alterations in the metabolome of each group. In the PCA score plot (Figure 5 A, B), the control groups and DOX groups were clearly divided into two clusters, which indicated that the CHF model was successfully prepared. In addition, the HG/[6]-GR and HG groups were significantly separated from DOX group and closer to the control group, especially the HG/[6]-GR group. Furthermore, to maximize the difference of metabolic profiles, PLS-DA analysis was carried out subsequently (Figure 5 C, D). The results showed that the PLS-DA models were verified by the class permutation and all these models had predictive ability with an R^2Y (cum), and Q^2 (cum). The corresponding value had been marked in the Figure 5 C-F. The R^2Y (cum) and Q^2Y (cum) were 0.999 and 0.992 in ESI+ mode, 0.998 and 0.971 in the ESI- mode, respectively. Also, the PLS-DA model was performed based on the DOX and HG/[6]-GR group (Figure

5 E, F). The DOX group could be clearly separated from the HG/[6]-GR group. The R^2Y (cum) and Q^2Y (cum) were 1 and 0.99 in the ESI+ mode, 0.997 and 0.963 in the ESI- mode, respectively. In addition, metabolic profile analysis between the DOX and HG or [6]-GR group in the positive mode and negative mode was also performed (Figure 6 A-D). Scatter plots of the control and DOX group, DOX and HG/[6]-GR group were shown in Figure 6 E-H, and scatter plots of the DOX and HG group, DOX and [6]-GR group were shown in Figure 6 I-L.

Table 1
mobile phases for metabolomics analysis.

T (min)	A (v/v)%	B (v/v)%
0 to 1.0	95	5
1.0 to 9.0	95 to 60	5 to 40
9.0 to 19.0	60 to 10	40 to 90
19.0 to 21.0	10 to 0	90 to 100
21.0 to 25.0	0	100

Notes: A: 0.1% formic acid in acetonitrile; B, 0.1% formic acid in water.

Identification and quantification of potential biomarkers

Next, differential metabolites in CHF treatment were identified. The variables that substantially contributed to the clustering and identification were identified when their VIP values ≥ 1.0 and |p(corr)| values ≥ 0.58 in S-plots. Finally, eight potential metabolites were expressed at significant levels and identified as biomarkers for the treatment of CHF. The basic information of these potential biomarkers was summarized in Table 3 with their corresponding name, formula, mass (m/z), retention time (min), and ratio changes (significance). Next, the mechanism of action of HG/[6]-GR on DOX induced CHF and the changes of eight possible metabolites were assessed and discussed. Compared with the control group, DOX substantially decreased peak area of acetylphosphate, 3-carboxy-1-hydroxypropylthiamine diphosphate, coenzyme A, PE(O-18:1(1Z)/20:4(5Z,8Z,11Z,14Z)), oleic acid, ans lysoPC(18:1(9Z)) (Figure 7A-E, 7G), but increase the peak area of PC(16:0/16:0) (Figure 7F) and palmitic acid (Figure 7H). Conversely, HG/[6]-GR could reverse these changes and decrease the peak area of PC(16:0/16:0) and palmitic acid. Notably, most of the metabolites indicated the formation of mitochondrial energy metabolism substrate. Besides, to determine the distribution and differences between groups, the clustering heat map and PCA were constructed based on the potential biomarker data (Figure 8B). Overall, the results indicated that HG/[6]-GR had obvious therapeutic effects on DOX-induced CHF. Especially, the curative effect of HG/[6]-GR group was better than that of HG and [6]-GR used alone (Figure 7).

tbody>

Table 2
Effect of DOX on cardiac function in rats.

Group	LVSP (mmHg)	LVEDP (mmHg)	$+dp/dt_{max}$ (mmHg/s)	$-dp/dt_{max}$ (mmHg/s)
C	108.13 ± 12.66	-4.59 ± 0.42	6653.83 ± 853.72	-4494.90 ± 574.24
DOX	18.9 ± 3.82**	-23.95 ± 10.26**	1990.14 ± 142.06**	-1301.12 ± 59.51**

C, control group; DOX, doxorubicin group. Compared with the control group, $^{**}P < 0.01$.

Table 3
Identified metabolites of the serum sample from different groups.

No	Compound Name	Formula	Mass (m/z)	Retention time (min)	Ratio changes (significance)	
					Control/DOX	HG/[6]-GR/DOX
1	Acetylphosphate	C_2H_5O5P	139.9872	20.01	4.57**	3.98##
2	3-Carboxy-1-hydroxypropylthiamine diphosphate	$C_{16}H_{25}N_4O_{10}P_2S$	527.0692	13.79	1.46**	1.48##
3	Coenzyme A	$C_{21}H_{36}N_7O_{16}P_3S$	767.1152	11.45	3.95**	3.54##
4	Palmitic acid	$C_{16}H_{32}O_2$	256.2402	16.37	0.39**	0.54##
5	PE(O-18:1(1Z)/20:4(5Z,8Z,11Z,14Z))	$C_{37}H_{66}NO_8P$	683.4375	20.46	3.57**	3.05##
6	Oleic acid	$C_{18}H_{34}O_2$	287.2819	7.84	3.30**	3.10##
7	LysoPC(18:1(9Z))	$C_{24}H_{51}NO_6P$	480.3086	15.87	1.85**	1.75##
8	PC(16:0/16:0)	$C_{46}H_{83}NO_8P$	808.5856	15.33	0.43**	0.64##

Compared with control group, $^{**}P < 0.01$; compared with DOX group, $^{\#\#}P < 0.01$.

Pathway analysis of CHF treatment

To explore the possible pathway of HG/[6]-GR and DOX intervention in CHF, the KEGG ID of endogenous metabolites was imported into the MetaboAnalyst 4.0 system for the pathway analysis and visualization. The results showed that CHF-related metabolites were responsible for energy metabolism pathway, including glycerophospholipid metabolism, biosynthesis of unsaturated fatty acids, fatty acid degradation, linoleic acid metabolism, alpha-Linolenic acid metabolism, glycosylphosphatidylinositol (GPI)-anchor biosynthesis, pantothenate and CoA biosynthesis, citrate cycle (TCA cycle), pyruvate metabolism, arachidonic acid metabolism, fatty acid elongation, fatty acid biosynthesis (Figure 8A). The match status, p value, -log(p) and the impact of each metabolic pathway were listed in Table 4. In addition, the relationship among metabolic pathways and metabolites was shown in the Figure 9C. The recovery trend of metabolites showed that the therapeutic effect of HG/[6]-GR on heart was related to the above eight metabolic biomarkers and twelve metabolic pathways. These results were consistent with the biochemical parameters and histological examination.

Table 4
Results of integrating pathway analysis with MetaboAnalyst 4.0.

No	Pathway Name	Match Status	*p*	-log(p)	Impact
1	Glycerophospholipid metabolism	3/36	0.00064401	7.3478	0.21631
2	Biosynthesis of unsaturated fatty acids	2/36	0.014161	4.2573	0
3	Fatty acid degradation	2/39	0.016523	4.103	0.12404
4	Linoleic acid metabolism	1/5	0.026263	3.6396	0
5	Alpha-Linolenic acid metabolism	1/13	0.067028	2.7026	0
6	Glycosylphosphatidylinositol (GPI)-anchor biosynthesis	1/14	0.072017	2.6308	0.00399
7	Pantothenate and CoA biosynthesis	1/19	0.096614	2.337	0.175
8	Citrate cycle (TCA cycle)	1/20	0.10146	2.288	0.08764
9	Pyruvate metabolism	1/22	0.1111	2.1973	0
10	Arachidonic acid metabolism	1/36	0.17603	1.7371	0
11	Fatty acid elongation	1/39	0.18939	1.6639	0
12	Fatty acid biosynthesis	1/47	0.2241	1.4957	0.01472

Discussion

Cardiomyocyte energy metabolism, especially fatty acid and glucose metabolism, changes in HF, and is considered to be a factor of heart function impairment in patients with HF.[22] Fatty acid β-oxidation is a process in which fatty acids decompose to produce ATP. In a series of steps of long-chain coenzyme A (COAs) entering mitochondria, COAs are converted into long-chain acyl coenzyme by carnitine palmitoyltransferase 1 (CPT1).[23] Long chain acyl CoA can enter into β-oxidation of fatty acids. One acetyl CoA is generated from each cycle by this pathway as well as NADH and FADH2. The NADH and FADH2 produced by β-oxidation of fatty acids and the TCA cycling of the acetyl CoA are used by electron transport chain for producing ATP.[24] In addition, the metabolism of fatty acids is an important energy source under the conditions of hunger, starvation, infection and diabetic ketoacidosis. In the state of CHF, the mitochondrial fatty acids metabolism is significantly impaired. In return, inhibition of fatty acid metabolism can cause myocardial insufficiency.[25,26]

The pharmacodynamic effects of HG/[6]-GR on CHF were systematically evaluated. Firstly, the multi-channel physiological signal detection system was used to evaluate the CHF model. The results showed that + dp/dt_{max} value had been reduced to 50% of the control group, indicating the successful preparation of CHF model. Secondly, the system was used to detect the therapeutic effect of HG/[6]-GR on CHF. Surprisingly, HG/[6]-GR could significantly increase the + dp/dt_{max} value of CHF rats, and their combination was similar to that of DH group. As serum BNP and NT-proBNP levels are the most widely used biomarkers in the diagnosis and treatment of HF, which are helpful for the diagnosis, differential diagnosis, risk stratification, efficacy monitoring and prognosis evaluation of acute-HF (AHF) and CHF.[27] Serum LDH, CK-MB, and AST levels can be used to evaluate whether the myocardium is damaged.[28] These parameters were comprehensively detected in the current study. The results showed that HG/[6]-GR could significantly reduce the increase of serum BNP, NT-proBNP, LDH, CK-MB, and AST

caused by DOX. Furthermore, combined with the results of cardiac histopathology and TUNEL staining, HG/[6]-GR could improve the changes of myocardial histopathology and reduce the apoptosis of cardiomyocytes. According to the results of pharmacodynamic study, HG/[6]-GR might have a significant therapeutic effect on DOX-induced CHF.

Our previous study has shown that HG in combination with [6]-GR can substantially increase the CPT-1 level decreased by DOX, which can relieve cardiomyocyte injury induced by DOX via regulating fatty acid metabolism in the TCA cycle based on cell metabolomics.[20] In the present study, serum metabolomics coupled with integrative pharmacology has further improved our understanding of the therapy of DOX induced CHF with HG/[6]-GR from several pivotal aspects.

In the present study, a UHPLC-Q-TOF/MS-based serum metabolomic approach was used to study serum metabolites changes in CHF. Moreover, we demonstrated the therapeutic effects of HG/[6]-GR against CHF in rats, which specifically caused a significant restoration of their myocardial metabolic profiles. This alteration laid the foundation for further investigation into the key mechanisms of HG/[6]-GR in the treatment of CHF. Eight metabolites were identified in the CHF treatment, including acetylphosphate, 3-carboxy-1-hydroxypropylthiamine diphosphate, coenzyme A, palmitic acid, PE(O-18:1(1Z)/20:4(5Z,8Z,11Z,14Z)), oleic acid, lysoPC(18:1(9Z)), and PC(16:0/16:0), which are distributed in twelve metabolic pathways. Most of the detected compounds are intermediates of energy metabolism. Among the changes of these potential metabolic pathways, the most obvious abnormality occurs in energy metabolism, which indicates that CHF is related to the disorder of energy metabolism in the heart. These finding are consistent with the previous studies.[29-31] Among these metabolites, acetylphosphate can phosphorylate biologically significant substrates in a way similar to ATP, promoting the origin of metabolism.[32] Coenzyme A is mainly involved in the metabolism of fatty acids and pyruvate, which can stimulate the tricarboxylic acid (TCA) cycle and provide 90% of the energy needed for the body's life.[33] Palmitic acid diets can cause lipotoxicity and energy metabolism imbalance in vivo and in vitro.[34] Specifically, Palmitic acid treatment can induce cardiomyocyte apoptosis, which is manifested by the appearance of apoptotic nucleus, the activation of caspase 3, the release of mitochondrial cytochrome C and the loss of mitochondrial cardiolipin.[35] Our results showed that DOX could substantially decrease the level of acetylphosphate and coenzyme A, but increase palmitic acid, indicating the damage to myocardial energy metabolism. Nevertheless, HG/[6]-GR could significantly reverse this change and affect the fatty acid metabolism and citrate cycle. As fatty acid metabolism is a notable mechanism for creating energy for the heart and a significant target for storing or creating energy for the heart,[36,37] HG/[6]-GR may play a crucial role in the treatment of CHF by improving the energy metabolism function of myocardial mitochondria.

In this study, although the effectiveness and potential mechanism of HG combined with [6]-GR in the treatment of CHF have been elucidated by a comprehensive method, some limitations still exists: (a) this study indicates that HG/[6]-GR may play a role in the treatment of CHF by affecting myocardial energy metabolism, the gene and protein expression of related pathways have not been verified to confirm the target mechanism of HG and [6]-GR; (b) the present study only discussed the effect of HG and [6]-GR on several biomarkers of metabolic difference, but the specific effect on other metabolites of tricarboxylic acid cycle remains to be elucidated; (c) in addition to myocardial energy metabolism, the causes of CHF include apoptosis and inflammation, whether HG and [6]-GR can play the role of CHF treatment through other channels remains to be studied; (d) the biomarkers of HG/[6]-GR affecting CHF have been discussed in serum metabolism level, how HG/[6]-GR affect these different biomarkers and what is the mode of action remains to be further studied. Therefore, although targeting mitochondrial energy

metabolism is a promising strategy for the treatment of CHF, further studies are needed to confirm the potential beneficial effect of regulating these metabolic targets as a method for the treatment of CHF.

Conclusion

The present study was to explore the therapeutic effect and possible mechanism of HG/[6]-GR in the treatment of CHF specifically induced by DOX and increase understanding of CHF based on the serum metabolomics. Compared with the control group, the myocardial metabolic spectrum of CHF rats was significantly altered. Furthermore, the difference metabolic markers of the control group, DOX group and HG/[6]-GR group were mainly involved in the cardiac energy metabolism. In addition, the cardiac function and histopathology of the HG/[6]-GR group were significantly ameliorated. The therapeutic effect of HG/[6]-GR might be attributed to its recovery of the disordered of mitochondrial energy metabolism pathway. These findings might provide novel insights for clarifying the potential mechanism of CHF and help to investigate the therapeutic effects and mechanism of HG/[6]-GR in the treatment of CHF.

Abbreviations

HG: higenamine; [6]-GR: [6]-gingerol; DOX: doxorubicin; CHF: chronic heart failure; CVD: cardiovascular disease; ACEI: angiotensin-converting enzyme inhibitors; TCM: traditional Chinese medicine; DH: dobutamine hydrochloride; ± dp/dtmax, left ventricular pressure max or min; LVEDP: left ventricular enddiastolic pressure; LVSP: left ventricular systolic pressure; BNP: brain natriuretic peptide; LDH: lactate dehydrogenase; CK-MB: creatine kinase-MB; AST: aspartate aminotransferase; HE: hematoxylin-eosin; TUNEL: terminal deoxynucleotidyl transferase dUTP nick end labeling; ESI: electrospray ionization; QC: quality control; PCA: principal component analysis; PLS-DA: partial least-squares discriminant analysis.

Declaration

Acknowledgements

The authors would like to thank all authors of references.

Funding

This research was supported by National Natural Science Foundation of China (81573631 and 81874365) and the National Key R&D Program of China (No. 2018YFC1704500)

Availability of data and materials

The data used to support the findings of this study are available from the corresponding author upon reasonable request.

Ethics approval and consent to participate

All animal procedures complied with the Guiding Principles for the Care and Use of Laboratory Animals of China and Institutional Animal Care and Use Committee of the Fifth Medical Center of PLA General Hospital.

Consent for publication

Not applicable.

Competing interests

The authors declare that this research was conducted in the absence of any commercial or financial relationships that could be construed as a potential conflict of interest.

Author Contributions

Jianxia Wen and Xiao Ma performed the experiments and wrote the manuscript. Ming Niu and Ying Huang collected and prepared samples. Junjie Hao and Ruilin Wang performed the analyses. Ruisheng Li analysed the data. Yanling Zhao and Jian Wang designed the study and amended the paper.

References

1. Benjamin EJ *et al*. Heart disease and stroke statistics-2019 update: a report from the American Hea3rt Association. *Circulation* 2019; 139: e56-e528.
2. Frank LD *et al*. Optimizing Management of Heart Failure by Using Echo and Natriuretic Peptides in the Outpatient Unit. *Adv Exp Med Biol - Advances in Internal Medicine* 2018; 3: 145-159.
3. Fernando ADA *et al*. Early warning systems for the management of chronic heart failure: a systematic literature review of cost-effectiveness models. *Expert Review of Pharmacoeconomics & Outcomes Research* 2018; 18: 161-175.
4. Desai A. Hyperkalemia associated with inhibitors of the renin-angiotensin-aldosterone system: balancing risk and benefit. *Circulation* 2008; 118: 1609-1611.
5. Thomas GL *et al*. New medical therapies for heart failure. *Nature Reviews Cardiology* 2015; 12: 730-740.
6. Wen JX *et al*. Protective effects of higenamine combined with [6]-gingerol against doxorubicin-induced mitochondrial dysfunction and toxicity in H9c2 cells and potential mechanisms. *Biomedicine & Pharmacotherapy* 2019; 115: 108881.
7. Sreekumar A *et al*. Metabolomic profiles delineate potential role for sarcosine in prostate cancerprogression. *Nature* 2009; 457: 910-914.
8. Nicholson JK *et al*. Systems biology: Metabonomics. Nature 2008; 455: 1054-1056.
9. Clayton TA *et al*. Pharmaco-metabonomic phenotyping and personalized drug treatment. *Nature* 2006; 440: 1073-1077.
10. Wei SZ *et al*. The modulatory properties of Li-Ru-Kang treatment on hyperplasia of mammary glands using an integrated approach. *Front Pharmacol* 2018; 9: 651.
11. Ji H *et al*. LC-MS based urinary metabolomics study of the intervention effect of aloe-emodin on hyperlipidemia rats. *J Pharm Biomed Anal* 2018; 156: 104-115.
12. Yang YX *et al*. Metabolomics profiling in a mouse model reveals protective effect of Sancao granule on Con A-Induced liver injury. *Journal of Ethnopharmacology* 2019; 238: 111838.
13. Wen JX *et al*. Therapeutic effects of Aconiti Lateralis Radix Praeparata combined with Zingiberis Rhizoma on doxorubicin-induced chronic heart failure in rats based on an integrated approach. *Journal of Pharmacy and Pharmacology* 2020; 72: 279-293.

14. Bai Y *et al*. Sulforaphane protection against the development of doxorubicin-induced chronic heart failure is associated with Nrf2 upregulation. *Cardiovasc Ther* 2017; 35: e12277.
15. Siveski-Iliskovic N *et al*. Probucol promotes endogenous antioxidants and provides protection against adriamycin-induced cardiomyopathy in rats. *Circulation* 1994; 89: 2829–2835.
16. Wen JX *et al*. Cardioprotective effects of Aconiti Lateralis Radix Praeparata combined with Zingiberis Rhizoma on doxorubicin-induced chronic heart failure in rats and potential mechanisms. *J Ethnopharmacol* 2019; 238: 111880.
17. Zhang L *et al*. Zingiberis rhizome mediated enhancement of the pharmacological effect of aconiti lateralis radix praeparata against acute heart failure and the underlying biological mechanisms. *Biomed Pharmacother* 2017; 96: 246–255.
18. Wen JX *et al*. Salsolinol has effect on attenuating doxorubicin-induced chronic heart failure in rats and improving mitochondrial function in H9c2 cardiomyocytes. *Fron Pharmacol* 2019; 10: 1135.
19. Lu X *et al*. The protective effects of compatibility of Aconiti Lateralis Radix Praeparata and Zingiberis Rhizoma on rats with heart failure by enhancing mitochondrial biogenesis via Sirt1/PGC-1a pathway. *Biomed Pharmacother* 2017; 92: 651–660.
20. Wen JX *et al*. Therapeutic effects of higenamine combined with [6]-gingerol on chronic heart failure induced by doxorubicin via ameliorating mitochondrial function. *Journal of Cellular and Molecular Medicine* 2020; 00: 1-15.
21. Chong, J *et al*. Using MetaboAnalyst 4.0 for Comprehensive and Integrative Metabolomics Data Analysis. *Current Protocols in Bioinformatics* 2019; 68: e86.
22. Murray JD *et al*. The effect of ribonucleotide reductase overexpression on cardiomyocyte metabolism. *Biophysical Journal* 2017; 112: 424a.
23. Ward AH *et al*. Metabolic support for the heart: complementary therapy for heart failure? *European Journal of Heart Failure* 2016; 18: 1420-1429.
24. Natasha F *et al*. Targeting mitochondrial oxidative metabolism as an approach to treat heart failure. *Biochimica et Biophysica Acta* 2013; 1833: 857-865.
25. Takahiro M *et al*. Effects of L-Carnitine on Propofol-Induced Inhibition of Free Fatty Acid Metabolism in Fasted Rats and in Vitro. *Open Journal of Anesthesiology* 2018; 8: 147-158.
26. Dolinsky VW. The role of sirtuins in mitochondrial function and doxorubicin-induced cardiac dysfunction, *Chem* 2017; 398: 955-974.
27. Piotr P *et al*. ESC guidelines for the diagnosis and treatment of acute and chronic heart failure 2016. *European Journal of Heart Failure* 2016; 1-121.
28. Zhang L *et al*. Functional metabolomics characterizes a key role for N-acetylneuraminic acid in coronary artery diseases. *Circulation* 2018; 137: 1374–1390.
29. Al-Hesayen A *et al*. Selective versus nonselective B-adrenergic receptor blockade in chronic heart failure: differential effects on myocardial energy substrate utilization, *J. Heart Fail* 2005; 7: 618–623.
30. Fukushima A *et al*. Myocardial Energy Substrate Metabolism in Heart Failure: from Pathways to Therapeutic Targets. *Curr Pharm Des* 2015; 21: 3654-3664.
31. Yang Y *et al*. Effects of PPARα/PGC-1α on the energy metabolism remodeling and apoptosis in the doxorubicin induced mice cardiomyocytes in vitro. *Int J Clin Exp Pathol* 2015; 8: 12216-12224.

32. Whicher A *et al*. Acetyl Phosphate as a Primordial Energy Currency at the Origin of Life. *Orig Life Evol Biosph* 2018; 48: 159-179.
33. Arata F *et al*. Myocardial energy substrate metabolism in heart failure: from pathways to therapeutic targets. *Current Pharmaceutical Design* 2015; 21: 3654-3664.
34. Chen YP *et al*. Palmitic acid interferes with energy metabolism balance by adversely switching the SIRT1-CD36-fatty acid pathway to the PKC zeta-GLUT4-glucose pathway in cardiomyoblasts. *Journal of Nutritional Biochemistry* 2016; 31: 137–149.
35. Leroy C *et al*. Protective effect of eicosapentaenoic acid on palmitate-induced apoptosis in neonatal cardiomyocytes. *Biochim Biophys Acta* 2008; 1781: 685-693.
36. Arad M *et al*. AMP-activated protein kinase in the heart: role during health and disease. *Circ Res* 2007; 100: 474-488.
37. Miller EJ *et al*. Macrophage migration inhibitory factor stimulates AMP-activated protein kinase in the ischaemic heart. *Nature* 2008; 451: 578-582.

Figures

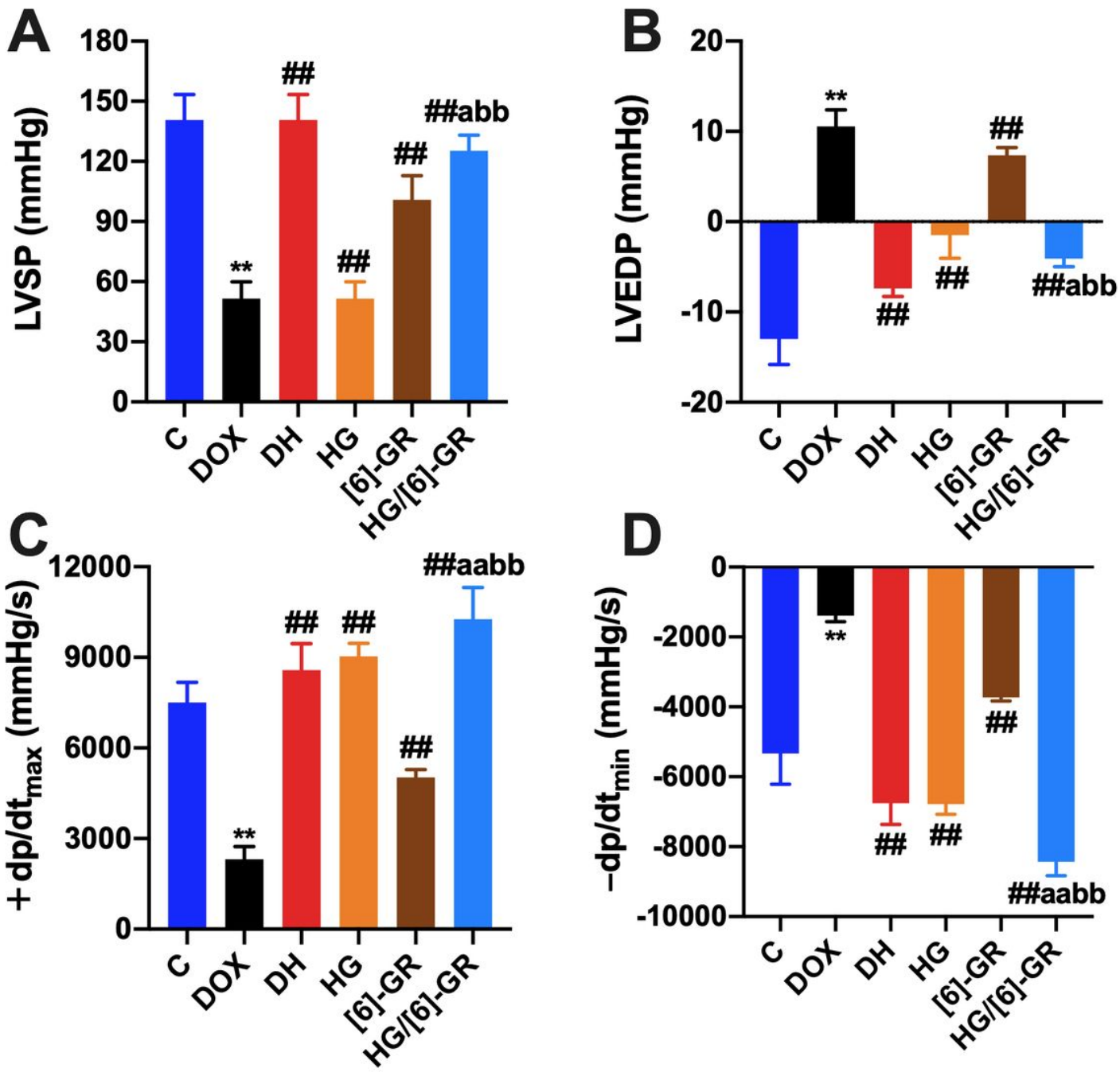

Figure 1

Effects of HG/[6]-GR on hemodynamic indices in rats. (A) LVSP; (B) LVEDP; (C) +dp/dtmax; (D) -dp/dtmax. Multichannel physiological signal acquisition system was used to detect hemodynamic parameters to reveal the ameliorating effects of HG/[6]-GR on myocardial function of CHF rats. Compared with the control group, **P < 0.01; compared with the DOX group, ##P < 0.01; compared with the HG group, aP < 0.05, aaP < 0.01; compared with the [6]-GR group, bbP < 0.01.

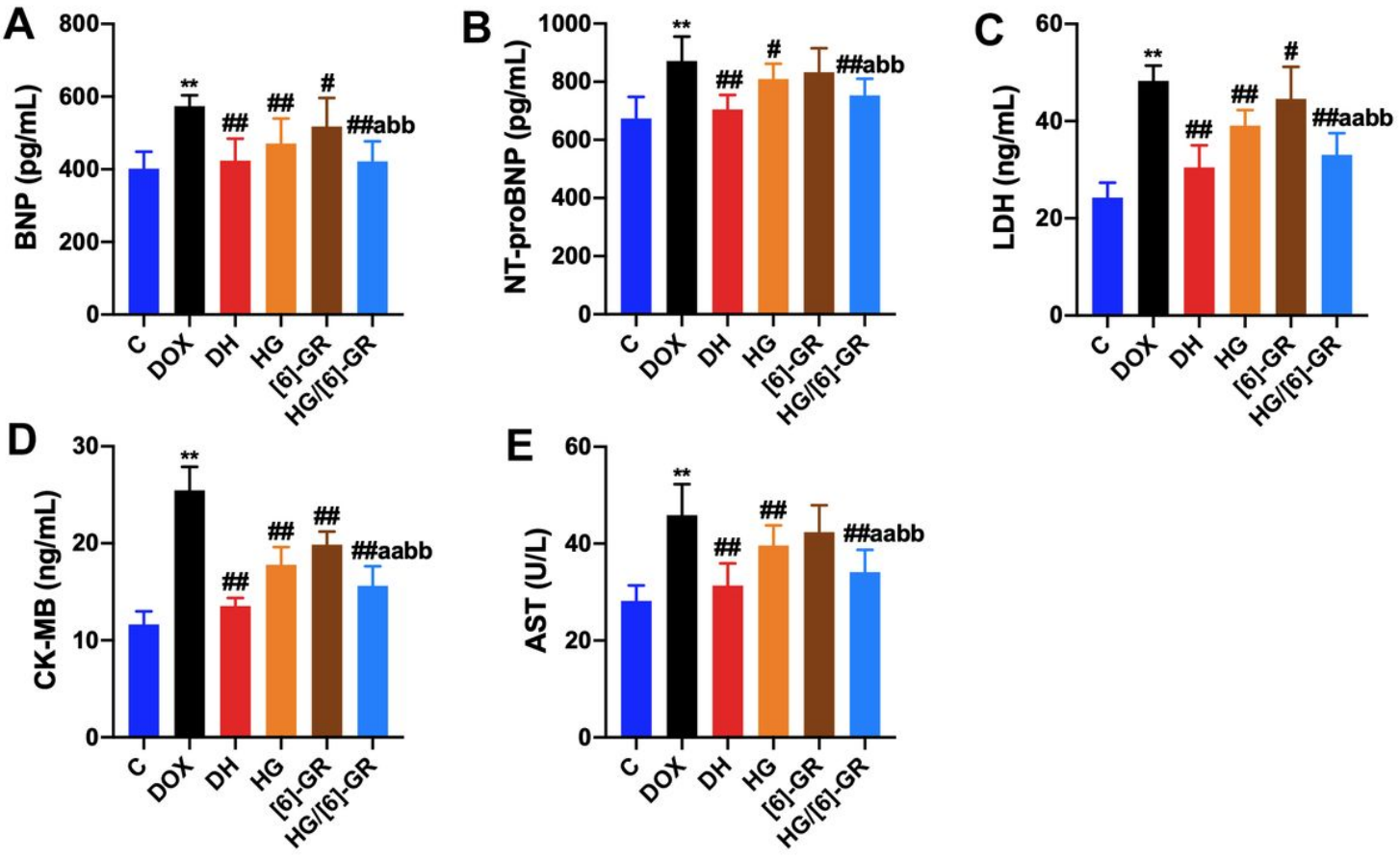

Figure 2

The serum levels of the myocardial biomarkers for the six groups. (A) BNP; (B) NT-proBNP; (C) LDH; (D) CK-MB; (E) AST. Compared with the control group, **P < 0.01; compared with the DOX group, #P < 0.05, ##P < 0.01; compared with the HG group, aP < 0.05, aaP < 0.01; compared with the [6]-GR group, bbP < 0.01.

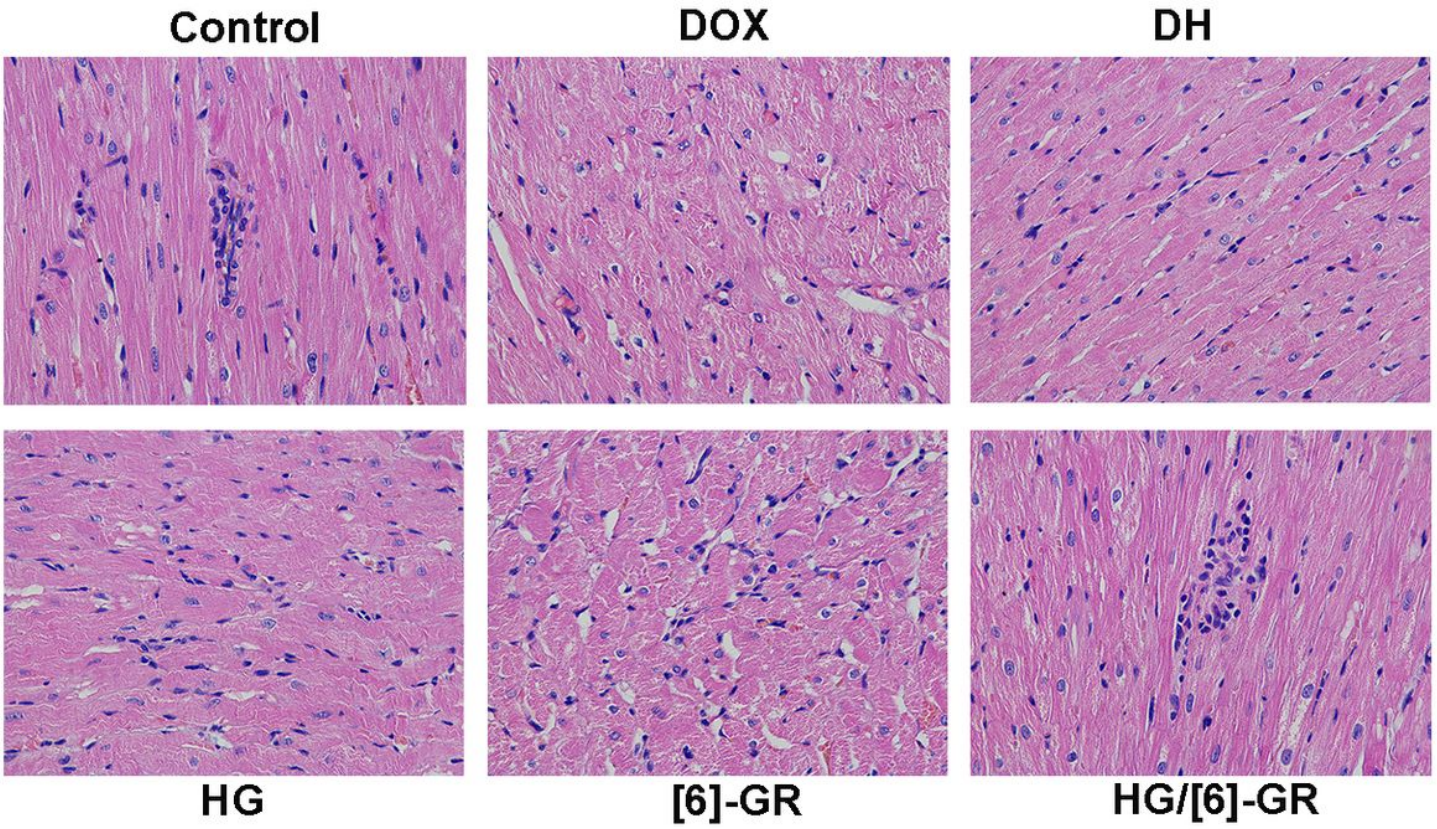

Figure 3

Effects of HG/[6]-GR on pathological changes of left ventricle in CHF rats (HE staining, 400 ×).

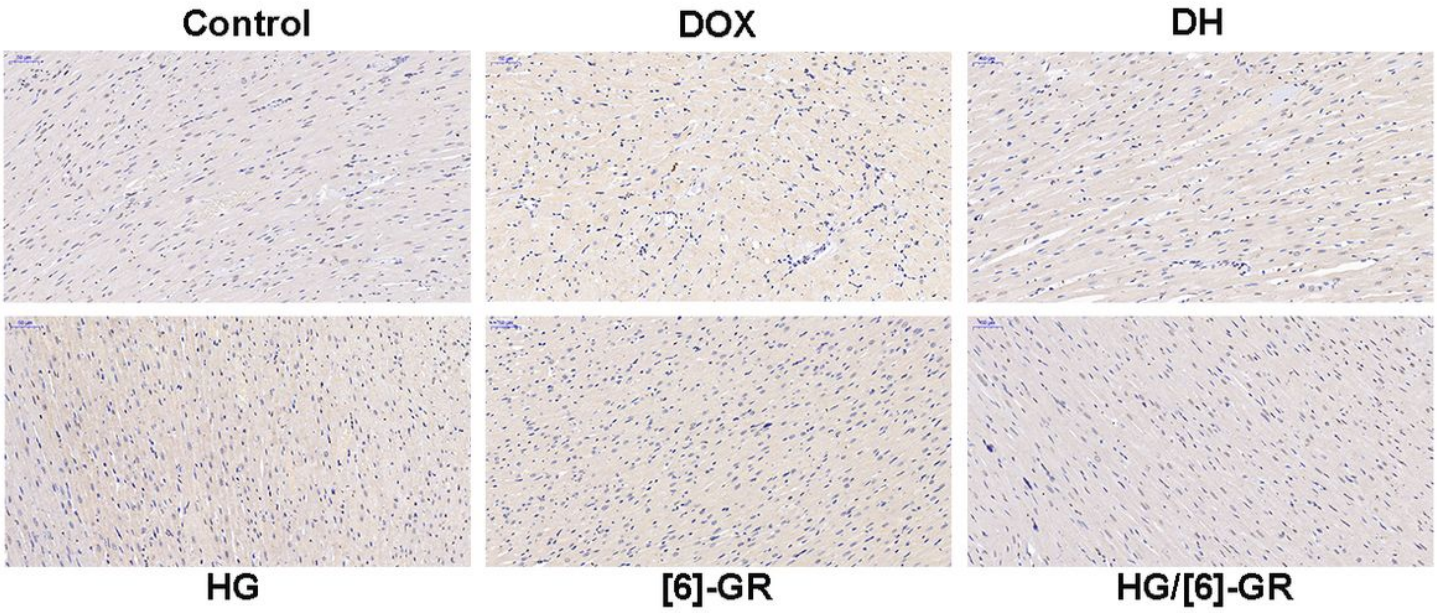

Figure 4

Effects of HG/[6]-GR on cardiomyocyte apoptosis of left ventricle in CHF rats (HE staining, 200 ×).

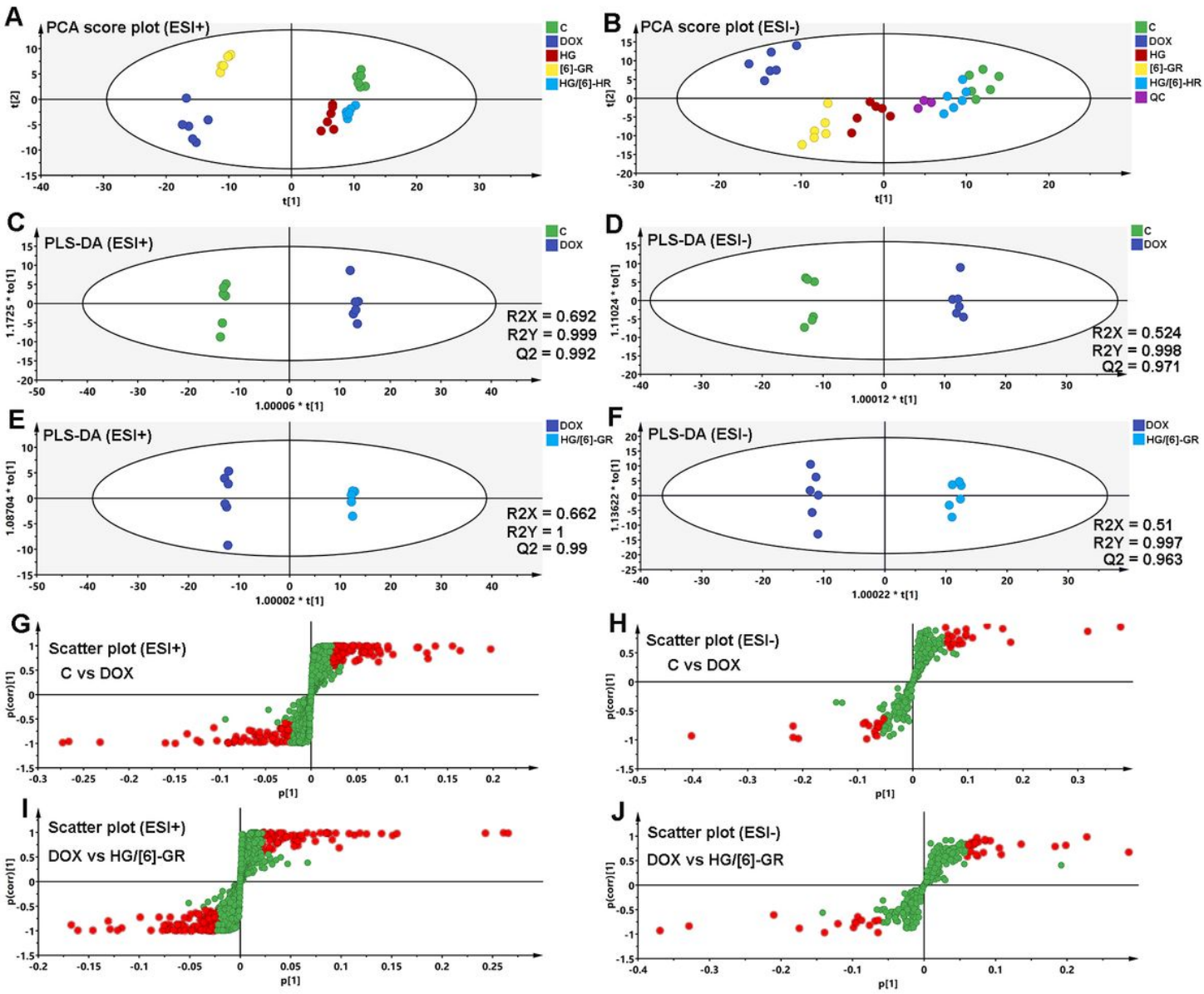

Figure 5

PCA and PLS-DA score plots of the serum samples from the control, DOX, and HG/[6]-GR groups. PCA score plots in the positive mode (A) and negative mode (B); PLS-DA score plots of control and DOX groups in the positive mode (C) and negative mode (D); PLS-DA score plots of DOX and HG/[6]-GR groups in the positive mode (E) and negative mode (F); Scatter plot of control and DOX groups in the positive mode (G) and negative mode (H); Scatter plot of DOX and HG/[6]-GR groups in the positive mode (I) and negative mode (J).

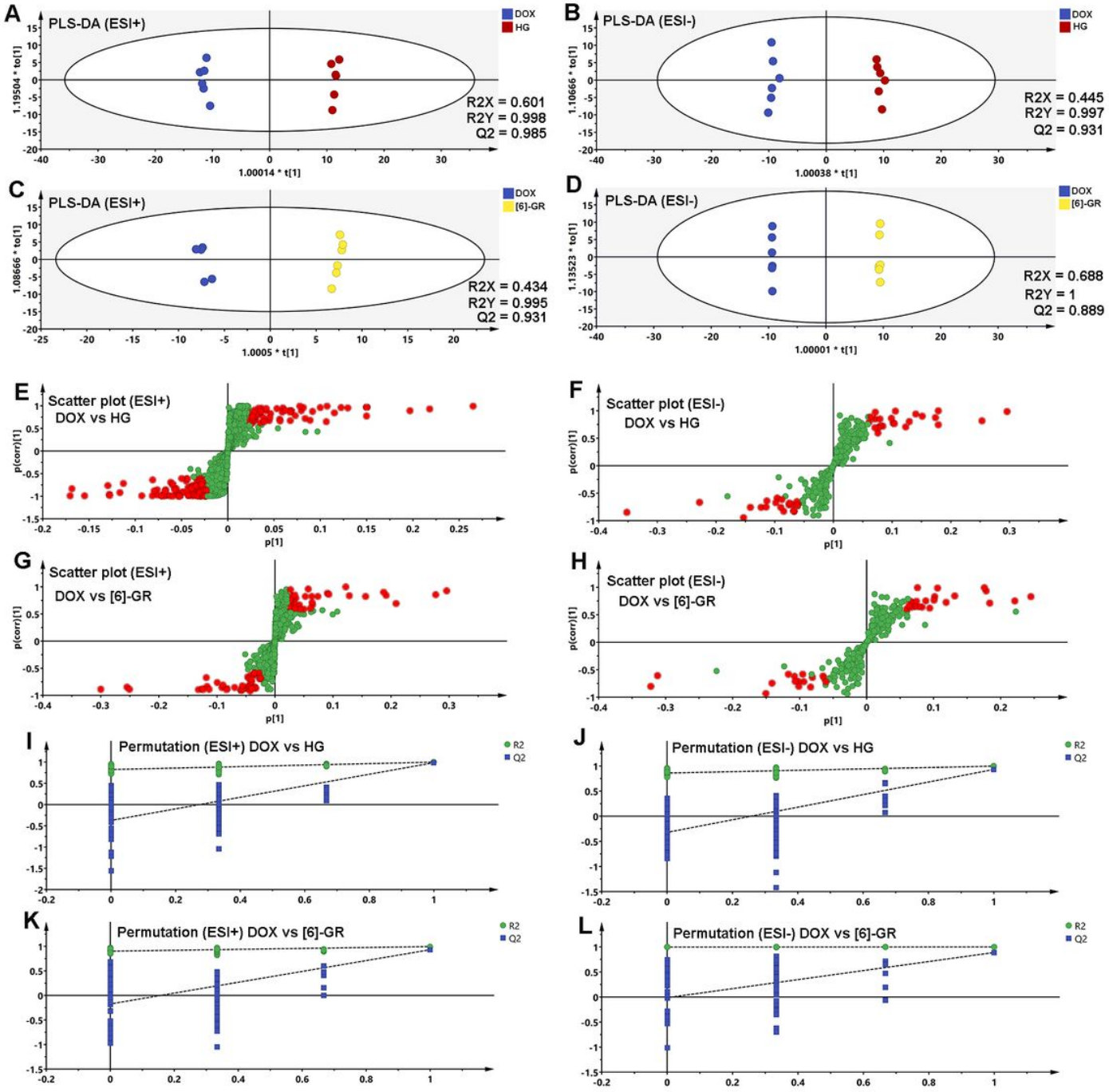

Figure 6

PLS-DA score plot, scatter plot, and 100 iteration permutation of the serum samples from the DOX, HG and [6]-GR groups. PLS-DA score plots of DOX and HG groups in the positive mode (A) and negative mode (B); PLS-DA score plots of DOX and [6]-GR groups in the positive mode (C) and negative mode (D); Scatter plot of DOX and HG groups in the positive mode (E) and negative mode (F); Scatter plot of DOX and [6]-GR groups in the positive mode (G) and negative mode (H); 100 iteration permutation tests of DOX and HG groups in the positive mode (I) and negative mode (J); 100 iteration permutation tests of DOX and [6]-GR groups in the positive mode (K) and negative mode (L).

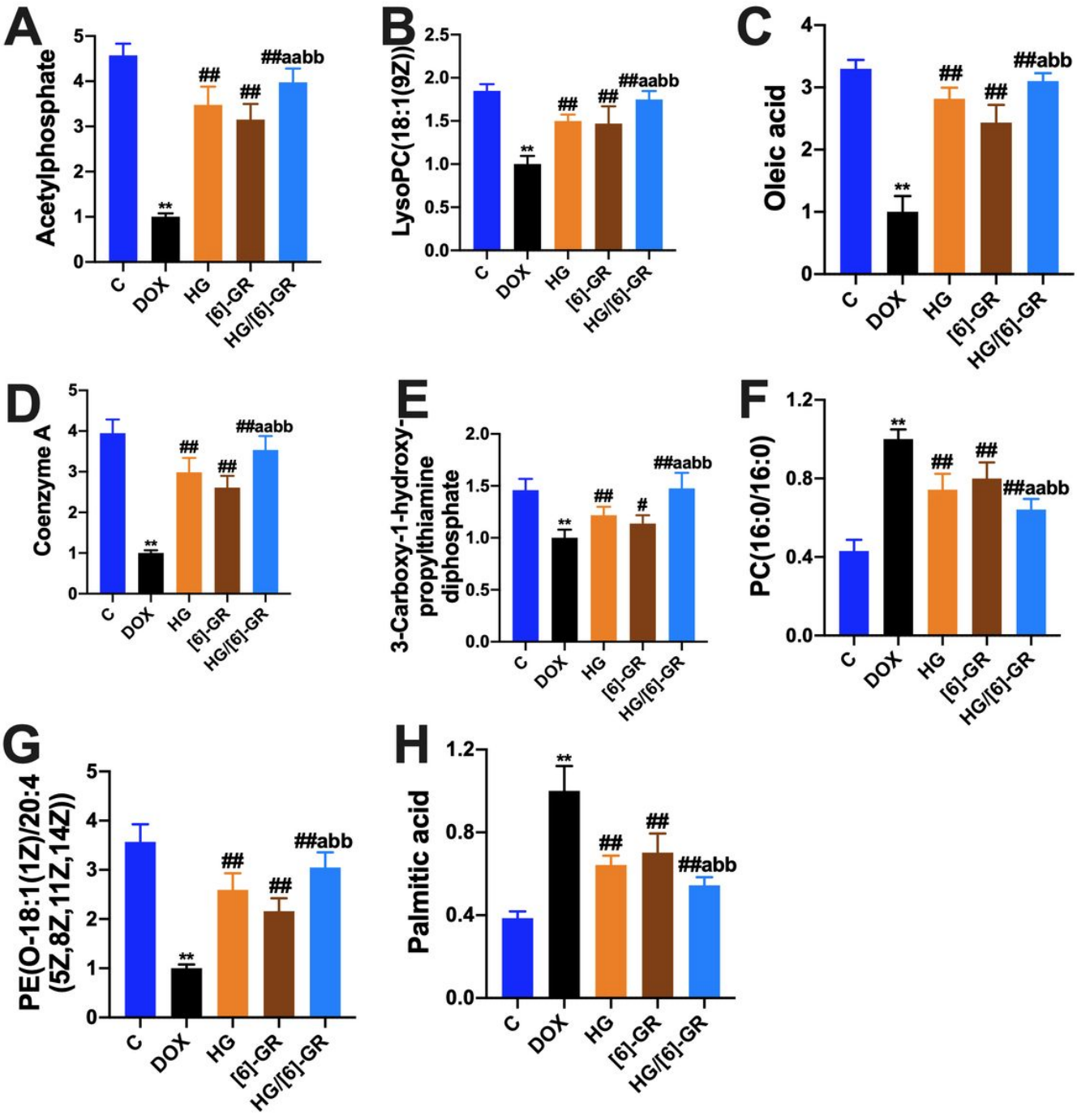

Figure 7

Potential biomarkers changes in DOX-induced CHF with HG/[6]-GR treatment. (A) Acetylphosphate; (B) LysoPC(18:1(9Z)); (C) Oleic acid; (D) Coenzyme A; (E) 3-Carboxy-1-hydroxypropylthiamine diphosphate; (F) PC(16:0/16:0); (G) PE(O-18:1(1Z)/20:4(5Z,8Z,11Z,14Z)); (H) Palmitic acid. Compared with the control group, **P < 0.01; compared with the DOX group, #P < 0.05, ##P < 0.01; compared with the HG group, aP < 0.05, aaP < 0.01; compared with the [6]-GR group, bbP < 0.01.

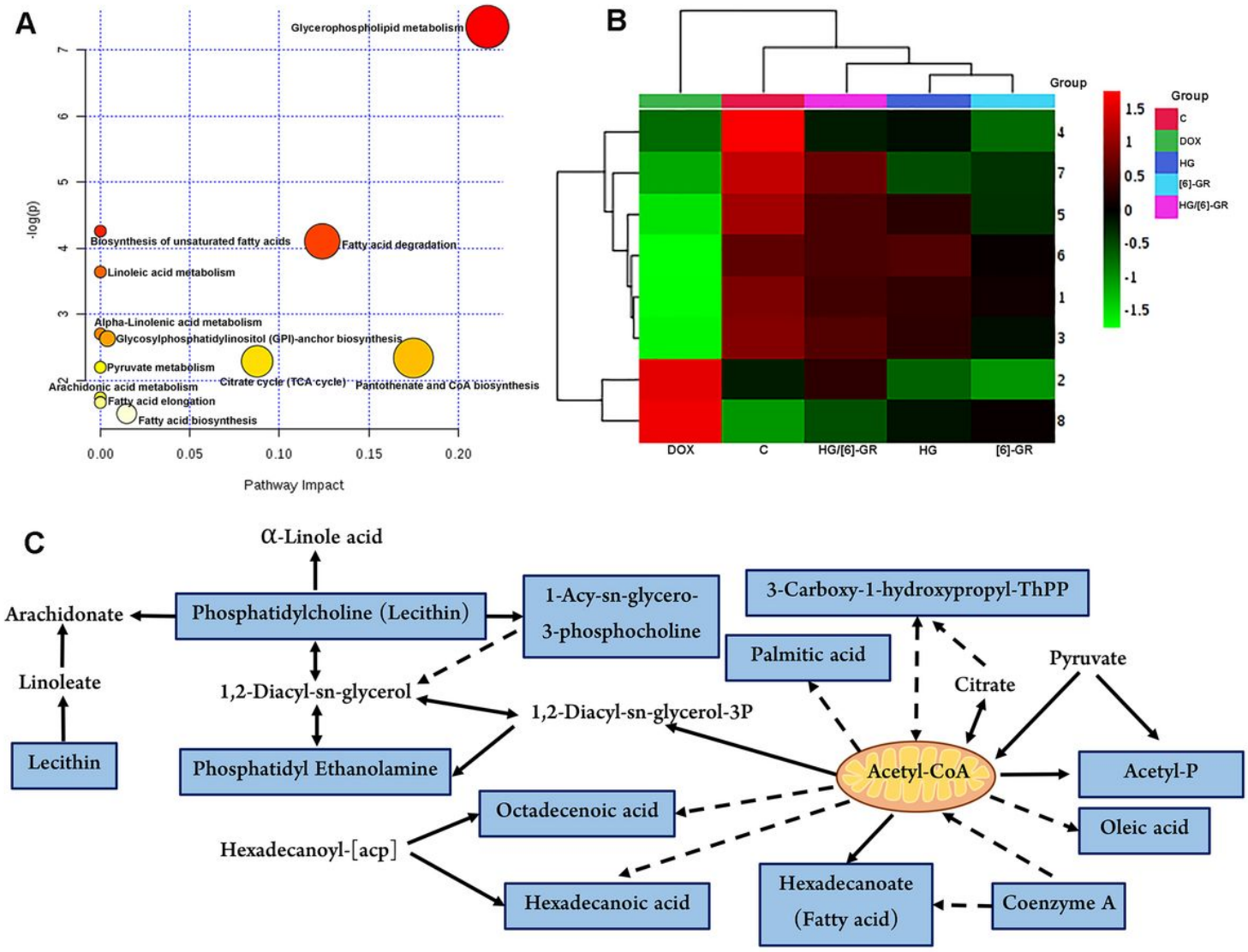

Figure 8

Metabolic biomarkers changes and related metabolic pathways involved in the treatment of HG/[6]-GR on CHF induced by DOX. (A) The metabolic pathways involved in the therapeutic effects of HG/[6]-GR on CHF; (B) The cluster heatmap of potential metabolites among groups. 1. Acetylphosphate; 2. 3-carboxy-1-hydroxypropylthiamine diphosphate; 3. coenzyme A; 4. palmitic acid; 5. PE(O-18:1(1Z)/20:4(5Z,8Z,11Z,14Z)); 6. oleic acid; 7. lysoPC(18:1(9Z)); 8. PC(16:0/16:0); (C) Relationship among the metabolic biomarkers and metabolic pathways.